QUANTITATIVE MORPHOLOGICAL CLASSIFICATION OF CRATERFORMS USING MULTIVARIATE OUTLINE-BASED SHAPE ANALYSIS. T.J. Slezak[1], J. Radebaugh[1], and E.H. Christiansen[1], [1]College of Physical and Mathematical Sciences, Department of Geological Sciences, Brigham Young University, Provo, UT 84602, (tjs@byu.edu).

Introduction: Craters formed by impact and volcanic processes are among the most fundamental planetary landforms. This study introduces multivariate, outline-based shape analysis as a quantitative tool to support the classification of planetary landforms. We adapt methods from modern studies in systematic evolutionary biology and paleontology used to identify or classify species by differences in form. Quantitative support for visual assessments of morphologic phenomena in geology enhance the scientific interpretations extracted from observations [1]. Both historical [2] and contemporary [3-4] works have stressed the importance of establishing a standardized quantitative classification system for the morphologic characterization of geologic landforms, yet no such system currently exists for the various types of craters formed on planets and moons. This study examines the morphology of terrestrial ash-flow calderas, terrestrial basaltic shield calderas, martian calderas, Ionian paterae, and lunar impact craters using quantitative, outline-based shape analysis and multivariate statistical methods to evaluate the differences between different types of craterforms. Ultimately, this should help establish relationships between the form and origin of craterforms.

Background: Shape is not easily quantified and communicating the information provided by morphology can be difficult. Existing methods used to differentiate landforms and assign respective nomenclature use criteria such as qualitative descriptions, indices derived from measurements (e.g., width to length ratio), and the fitting of mathematical models (e.g., power laws, quadratic equations) to evaluate landforms using morphologic variables [5]. Modern craterform studies apply techniques of traditional morphometrics [6-8] and directly link measurement-derived quantitative indices to geologic information and interpretations (e.g., [9-10]). These procedures use scalar measures such as area, perimeter, diameter, and depth, to compute values such as circularity (form factor), ellipticity, and depth-to-diameter ratio, which are used as primary quantitative descriptors of shape or form. However, these methods do not include the detailed spatial information inherent to complex or irregular geometry often present in natural geologic forms [11].

Methodology: The shapes of terrestrial ash-flow calderas, terrestrial basaltic shield calderas, martian calderas, Ionian paterae, and lunar impact craters were quantified using elliptic Fourier analysis (EFA) [12-13] and the Zahn and Roskies (Z-R) shape function [14]. A stereographic map projection is applied to each craterform image on which outlines were traced. Outlines were digitized by placing points along the bounds of an imaged craterform using the tpsDig2 software [15]. Next, the outline was interpolated to 99 equidistantly-spaced points and points are extracted as Cartesian coordinates.

The shapes, as sets of Cartesian coordinates, were rotated the point corresponding to the maximum distance from each shape's centroid. Quantities obtained from EFA are coefficients produced from a decomposition of the Fourier series for the shape, each harmonic order yields four coefficients. Higher order harmonics produce more precise approximations of shape (Fig. 1) at the cost of the inclusion of additional coefficients. The shape descriptors extracted from Z-R analysis are the angular deviation of the shapes from a circle. For 99 outline points, 98 values (in radians) are computed for each shape. The multivariate quantities produced by the Z-R function and the coefficients of the 2^{nd} to 10^{th} harmonics from EFA were subjected to discriminant analysis, to examine the maximum differences between the craterform groups and construct

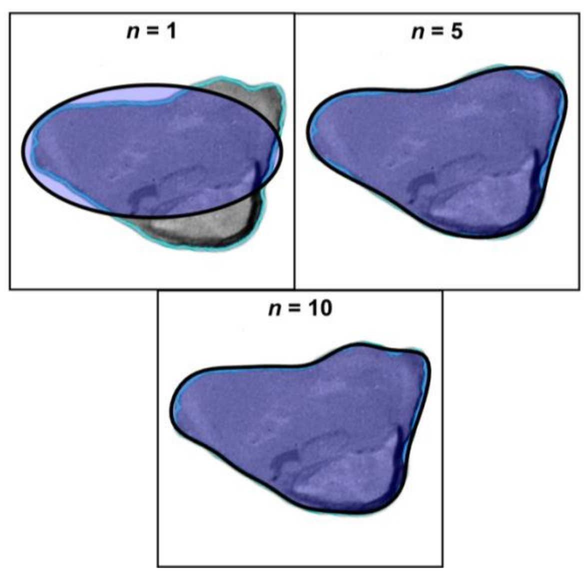

Figure 1. ***Shape approximation using higher harmonic orders of coefficients from EFA applied to the shape of Maasaw patera.***

a model to predict group membership using a classification function.

Results: Discriminant analysis of elliptic Fourier coefficients from the 2nd to the 10th harmonic and Z-R shape function datasets show that ash-flow calderas and paterae on Io are most similar in shape, as are basaltic shield calderas and martian calderas.

The model resulting from discriminant analysis assigns group membership to different types of craters. The shape classification model resulting from discriminant analysis of the EFA coefficients from the 2nd to 10th harmonic produces a 90.4% overall rate of success in group membership assignment among the craterforms. The classification results of this model for each group, as shown by Table 1 and Table 2, correctly identifies 138 of 154 (90%) of Ionian paterae and 154 of 155 (99%) of lunar impact craters from all craterforms in the study. The model also correctly classifies 31 of 35 (89%) of terrestrial basaltic shield calderas, 32 of 38 (84%) terrestrial ash-flow calderas, and 12 of 24 (50%) of martian calderas.

Table 1. ***Craterform classification rates of success from discriminant analysis of EFA coefficients.***

	Predicted Count					
Group	**Ash-Flow**	**Basaltic Shield**	**Io Patera**	**Lunar Impact**	**Mars Caldera**	**Count**
Ash-Flow	**84%**	0%	13%	3%	0%	100%
Basaltic Shield	0%	**89%**	0%	11%	0%	100%
Io Patera	1%	1%	**90%**	8%	0%	100%
Lunar Impact	0%	0%	1%	**99%**	0%	100%
Mars Caldera	0%	0%	25%	25%	**50%**	100%

The shape classification model resulting from discriminant analysis of the Z-R function values produces an 84.2% overall rate of success in group membership assignment among the craterforms. The classification results of this model for each group, as shown by Table 3 and Table 4, correctly identifies 148 of 154 (96%) of Ionian paterae and all lunar impact craters from the other craterforms. The model successfully classifies 18 of 35 (51%) of terrestrial basaltic shield calderas, 15 of 24 (63%) martian calderas, and only 6 of 38 (16%) terrestrial ash-flow calderas.

Table 2. ***Craterform classification rates of success from discriminant analysis of Z-R function output.***

	Predicted Count					
Group	**Ash-Flow**	**Basaltic Shield**	**Io Patera**	**Lunar Impact**	**Mars Caldera**	**Count**
Ash-Flow	**16%**	11%	13%	0%	61%	100%
Basaltic Shield	0%	**51%**	14%	0%	34%	100%
Io Patera	0%	0%	**96%**	4%	0%	100%
Lunar Impact	0%	0%	0%	**100%**	0%	100%
Mars Caldera	0%	17%	13%	8%	**63%**	100%

In contrast to the EFA classification model, the Z-R model successfully classifies more ionian patera and impact craters but performs poorly at classifying the other craterform groups. This result shows that the quantities communicate different shape information. The Z-R model is robust in its ability to classify end-members of shape complexity while the EFA model is robust in its ability to reliably classify among more groups.

Conclusion: Multivariate statistical analysis and classification models reveal that basalt shield calderas on Earth and Mars are similar in shape. This reflects our current understanding of the similarity in formation processes and compositions of these landforms. Furthermore, the models find that paterae on Io are most similar in shape to terrestrial ash-flow calderas. Both have relatively complex shapes. Perhaps these landforms have undergone equally complex formation or modification processes stemming from involvement of collapse, incremental growth, volatiles, large size, or other magma reservoir related factors. This study reveals multivariate statistical analyses can be effective tools for analyzing landforms on planetary surfaces. With larger datasets, a well-trained model has significant potential to reveal clues about the formation and variables involved in the genesis of landforms and enhance existing inferences for surface evolution and the geologic history of planetary bodies.

References: [1] MacLeod N. (2002) Earth Sci. Rev., 59, 27-47. [2] Evans I.S. (1972) Spatial Analysis in Geomorph., 17-90. [3] Pike R.J. (2001) Interpreting Remote Sensing Imagery, 83-114. [4] Mahanti P. et al. (2014) Icarus, 241, 114-129. [5] Evans I.S. (1986) Intl. Geomorph., 2, 105-124. [6] Lohmann G.P. (1983) Math. Geo., 15, 6, 659-672. [7] Rohlf F.J. and Marcus L.F. (1993) Trends Eco. Evo., 8, 129-132. [8] Lestrel P.E. 2000. Morphometrics for the Life Sciences, 284. [9] Fassett C.I. et al. (2009) Earth Plan. Sci. Let., 285, 297–308. [10] Michalski J.R. and Bleacher J.E. (2013) Nature, 502, 47-52. [11] MacLeod N. (1999) Paleobio. 25(1), 107-138. [12] Kuhl R. and Giardina C.R. (1982) Comp. Graph. Image Proc., 18, 236–258. [13] Ferson S. et al. (1985) Syst. Zoo., 34, 59. [14] Zahn C.T. and Roskies R.Z. (1972) IEEE Tran., Comp., C-21, 269-281. [15] Rohlf F.J. (2002) tps Software Series.